An Open-Source OpenSim Oculomotor Model for Kinematics and Dynamics Simulation

Constantinos Filip, Dimitar Stanev[1], and Konstantinos Moustakas

July 10, 2018

[1]Electrical and Computer Engineering Department, University of Patras, Greece; Corresponding author: stanev@ece.upatras.gr

Abstract

Studying human eye movements has significant implications for improving our understanding of the oculomotor system and treating various visuomotor disorders. An open-source musculoskeletal model of the human eye, that can be used for kinematics and dynamics analysis, is implemented based on the data reported in literature and made publicly available[1]. The model is implemented in `OpenSim`, which is an open-source framework for modeling and simulation of musculoskeletal systems. The calibration of the model parameters is based on physiological measurements of the human eye. The model incorporates an eye globe, orbital suspension tissues and six extraocular muscles. The excitation and activation patterns for a variety of targets can be calculated using the proposed closed-loop fixation controller that drives the model to perform saccadic movements in a forward dynamics manner. The controller minimizes the error between the desired saccadic trajectory and the predicted movement. Consequently, this model enables the investigation muscle activation patterns during static fixation and analyze the dynamics of various eye movements.

[1] SimTK project: https://simtk.org/projects/eye

Introduction

Rapid and accurate eye movements are crucial for coordinated direction of gaze Lee and Terzopoulos (2006). Studying human eye movement has significant implications for improving our understanding of the oculomotor system and treating visuomotor disorders. Over the past decades, biomechanics simulation has provided the means to analyze different human movements Delp et al. (2007). The same principles can be used to analyze visual tasks by modeling the musculoskeletal properties of the oculomotor system. Consequently, this model can be used to investigate muscle activation patterns during static fixation, analyze the dynamics of various eye movements, calculate metabolic costs and simulate eye disorders, such as different forms of strabismus. Furthermore, it can be easily integrated with available full body models in order to analyze the relation between the vestibular and oculomotor systems.

Saccadic movements are a generated from a coordination of the six Extraocular Muscles (EOMs). Clinical trials have provided a profound knowledge on the properties of the EOMs and their line of action on the eye globe Robinson et al. (1969), the resistive tension of the surrounding tissues Collins et al. (1981) and the length-tension relationship of the muscles Iskander et al. (2018). Various computational models of the extraocular muscles and orbital mechanics have been proposed, which provide insight and scientific bases for oculomotor biomechanics, control of eye movement and binocular misalignment. These models focus on the realism of muscle behavior and they were based on the viscoelastic properties and physiological data EOMs.

The first 3D biomechanical model was developed by Robinson (1964); Robinson and Fuchs (1969), who simplified the formulation by only considering the elasticity of the EOMs ignoring their dynamics. The model incorporates anatomically realistic muscle paths and empirical innervation-length-tension relationships. To study the neural control of rapid saccadic movements, models using anatomical and mechanical properties of EOMs have been developed by accounting for the nonlinear muscle dynamics Thelen et al. (2003); Millard et al. (2013). Such models, having the advantage of supporting dynamics simulation, are used in conjunction with brain level controllers James et al. (2018).

Methods

Eye Modeling

The orbital plant consists of the globe (eyeball), three pairs of extraocular muscles and the connective passive tissues. The size of an emmetropic human adult eye is approximately 0.0242 m (transverse, horizontal), 0.0237 m (sagittal, vertical), 0.022–0.0248 m (axial, anteroposterior) with no significant difference between sexes and age groups. In the transverse diameter, the eyeball size may vary from 0.021 m to 0.027 m. Thus, it can be approximated by a solid sphere with 0.012 m radius. The eyeball was constructed in `Blender`, using a spherical mesh with 32 segments and 12 rings, to construct the vitreous humor (body) as solid sphere and a conical plate to construct the cornea. The weight of an average human eye is 0.0075 kg and the moment of inertia can be calculated similarly as in the case of a spherical homogeneous and isotropic object with ($\boldsymbol{I} = 2/5mr^2$ at the center of mass).

Muscle Modeling

The six EOMs, including four rectus muscles and two oblique muscles, are controlled by the cranial nerves so as to track a visual target and to stabilize the image of the object. The Lateral Rectus (LR) and Medial Rectus (MR) muscles form an antagonistic pair that produce horizontal eye movements. The Superior Rectus (SR) and Inferior Rectus (IR) muscles form the vertical antagonist pair, which mainly controls vertical eye movement and also affects rotation about the horizontal plane and the line of sight (secondary action) due to insertion positions. The Superior Oblique (SO) muscle passes through the

cartilaginous trochlea attached to the orbital wall, which reflects the SO path by 51 deg. The Inferior Oblique (IO) muscle originates from the orbital wall anteroinferior to the globe center and inserts on the sclera posterior to the globe equator. The primary actions of SO and IO cause rotation of the globe around the visual axis and vertical movement.

The model relies on the passive pulley assumption in order to keep it simple and provide faster simulation speed. Table 1 shows the positions of muscle pulleys, as well as the origin and insertion points of the EOMs, defined in the local body coordinates of the globe. The data is based on physiological measurements Iskander et al. (2018), with some minor adaptation so as to prevent unrealistic penetration into the eye globe. Since no position was documented for the origin of the SO, a point close to the origins of the rectus muscles was chosen to match the fiber length in the primary position of the SO muscle.

Table 1: Muscle path points for the six EOMs (dimensions are given in meters).

Muscle	**Origin**			**Pulley**			**Insertion**		
	Ox	***Oy***	***Oz***	***Px***	***Py***	***Pz***	***Ix***	***Iy***	***Iz***
LR	-0.034	0.0006	-0.013	-0.0102	0.0003	0.012	0.0065	0	0.0101
MR	-0.030	0.0006	-0.017	-0.0053	0.00014	-0.0146	0.0088	0	-0.0096
SR	-0.0317	0.0036	-0.016	-0.0092	0.012	-0.002	0.0076	0.0104	0
IR	-0.0317	-0.0024	-0.016	-0.0042	-0.0128	-0.0042	0.00805	-0.0102	0
SO	0.0082	0.0122	-0.0152	-0.030834	0.001145	-0.01644	0.0044	0.011	0.0029
IO	0.0113	-0.0154	-0.0111	-0.00718	-0.0135	0	-0.008	0	0.009

The Millard muscle model Millard et al. (2013) has been adopted for the modeling of the EOMs, which permits parameterization of the Force-Length (F-L) curves according to the experimental measured data. The muscles were modeled using the rigid tendon assumption that ignores the elasticity of the tendon. This means that the series element of the muscle model is not included (the tendon length l^T is equal to the tendon slack length l_s^T). This assumption is valid when the ratio of the tendon length to the muscle length is less or equal to one. EOMs are considered parallel-fibered muscles, so the pennation angle is zero ($\alpha = 0$). The values for the maximum isometric force f_o^M, optimal fiber length l_o^M and tendon length l^T are presented in Table 1.

The active and passive F-L curves for the EOMs differ from that of a skeletal muscle. As shown in Figure 1, we can fine-tune these curves so as to fit the experimental data available for the LR muscle. The following values where used for the active (Table 2) and passive F-L curves.

The parameters that describe the above relationships were chosen to fit the curves reported in Iskander et al. (2018), by matching the F-L relationship at maximum activation of the LR muscle. This represents the first part of testing the fidelity of the model. Due to lack of data describing the other muscles, we used the parameters describing the normalized curves of active and passive F-L relationships of

Table 2: Parameters of the active F-L curve of the Millard muscle model.

Parameter	**Value**
min norm active fiber length	0.55
transition norm fiver length	0.7
max norm active fiver length	1.8
shallow ascending slope	2.4
minimum value	0.0

Table 3: Parameters of the active F-L curve of the Millard muscle model.

Parameter	**Value**
strain at zero force	-0.18
strain at one norm force	0.4

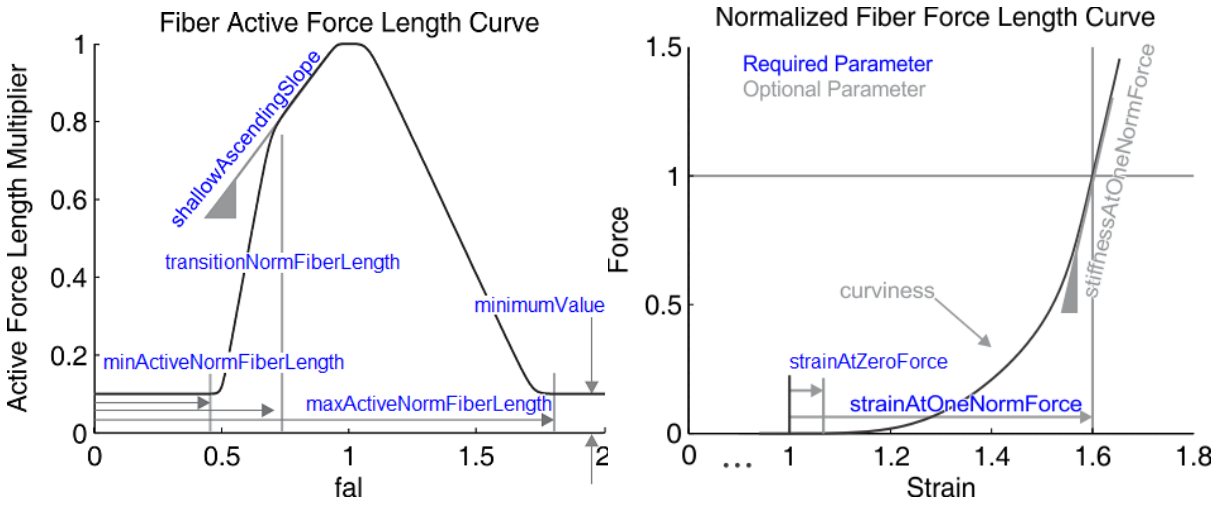

(a) Active F-L curve **(b)** Passive F-L curve

Figure 1: The active and passive F-L curve definition for the Millard muscle model as implemented in `OpenSim`.

the LR for the rest of the EOMs.

EOMs have a higher fraction of fast twitch fibers and thus different Force-Velocity (F-V) behavior, due to different structures compared to skeletal muscles. Despite that, the default Millard F-V curve was used for the six EOMs, since the behavior of the selected muscle model depends mainly on the maximum contraction velocity $v^{\max}$. The maximum muscle contraction velocity is tuned so as to match the peak velocity of saccadic eye movement $\omega^{\max} = 15.7$ rad / s (900 deg / s). Following this definition, the maximum muscle contraction velocity is given in optimal fiber length per seconds and it is thus different for each EOMs, as their optimal fiber length is different ($v^{\max} = \omega^{\max} r / l_o^M$). Furthermore, because of the different structure of neural control of the eyes, activation and deactivation delays ($\tau_d = 5$ ms) are lower than in skeletal muscles. Finally, two separate wrapping spheres for the rectus muscles and the oblique muscles were created, to avoid abnormal changes on the F-L curve as the eyeball rotates.

Table 4: Millard muscle parameters for the EOMs.

Muscle	Maximum Isometric Force (N)	Optimal Fiber Length (m)	Tendon Slack Length (m)	Maximum Contraction Velocity (m / s)
LR	1.4710	0.04898	0.0084	3.8483
MR	1.5740	0.04084	0.0038	4.6155
SR	1.1768	0.04487	0.0054	4.2009
IR	1.4269	0.04549	0.0048	4.1437
SO	0.6031	0.03956	0.0265	4.7648
IO	0.5590	0.04110	0.0015	3.5863

Passive Connective Tissues

The passive connective tissues apply a restoring force, which brings the globe back to the central position when the net force from the EOMs is zero. These tissues include all non-muscular suspensory tissues, such as Tenon's capsule, the optic nerve, the fat pad and the conjunctiva. The force-displacement curve

of the net elasticity can be represented as

$$\boldsymbol{f}_t = -k_p \boldsymbol{q} - k_c 10^{-3} \boldsymbol{q}^3 - k_d * \dot{\boldsymbol{q}} \tag{1}$$

where, $\boldsymbol{f}_t$ is the passive tissue forces, $k_p = 0.002225$ N m / rad, $k_c = 34.5297$ N m / (rad^3) and $k_v = 0.002$ N m s / rad the constants and $\dot{\boldsymbol{q}} \in \Re^3$ the rotational coordinates of the model Collins et al. (1981). These forces are modeled using `OpenSim`'s expression based coordinate force.

Results

Fixation Controller

A fixation controller was implemented as a custom `OpenSim` plugin. The parameters of the controller are: the desired horizontal θ_H and vertical θ_V fixation angles (in degrees), the saccade onset and velocity (in degrees), and the gains of Proportional Derivative (PD) tracking controller (k_p, k_d). A sigmoid function is used for generating smooth saccade trajectories

$$\begin{aligned} \theta_d(t) &= \frac{a}{2}(\tanh(b(t - t_0)) + 1) \\ \dot{\theta}_d(t) &= \frac{ab}{2}(\tanh^2(b(t - t_0)) - 1) \end{aligned} \tag{2}$$

where $\theta_d(t)$ and $\dot{\theta}_d(t)$ represent the desired orientation and velocity at time t, a the magnitude of the trajectory, b the slope and t_0 a time shift constant. Provided a fixation goal θ_g, a desired saccade velocity $\dot{\theta}_g$ and a saccade onset t_g the parameters of the sigmoid function are defined as follows $a = \theta_g$, $b = 2\dot{\theta}_g/\theta_g$ and $t_0 = t_s$. The PD tracking controller has the following form

$$\ddot{\theta}(t) = k_p(\theta_d(t) - \theta(t)) + k_d(\dot{\theta}_d(t) - \dot{\theta}(t)). \tag{3}$$

The sign and magnitude of $\ddot{\theta}(t)$ both for the horizontal and vertical displacement of the fixation target is used to actuate the corresponding muscles in order to achieve the desired goal. Figure 2 presents an instance of the model during simulation with the corresponding muscles activated. Figure 3 depicts the simulated coordinates, speeds and estimated EOMs activations that reproduce the desired saccade trajectory.

Conclusion

A realistic oculomotor model representing the motility of a normal human eye was presented and made publicly available. The parameters of the model were calibrated using available experimental measured data. The model can be used for kinematics and dynamics analysis or as a tool for obtaining the muscle activations that generate a desired saccade, using a closed-loop fixation controller in a Forward Dynamics (FD) manner. There is of course space for further improvement, which will enhance the accuracy and the predictability of the proposed computational model. In this study, we didn't attempt to model the muscle pulleys Kono et al. (2002), which vary as a function of the model coordinates. Therefore, the users should consider performing further validation of the eye model based on the requirements of the targeted utility and the variables of interests.

Figure 2: Model with a fixation at $\theta_H = -15$ deg $\theta_V = 15$ deg during simulation. Blue denotes low and red high muscle activation levels.

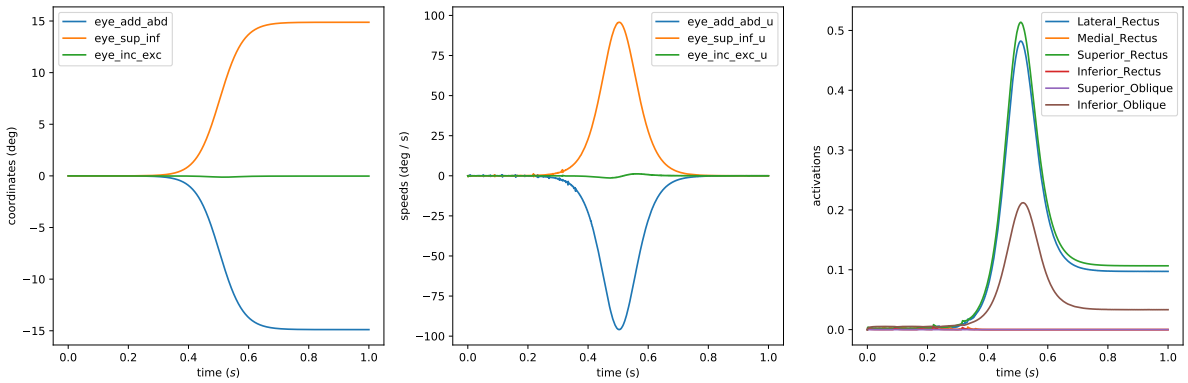

Figure 3: Simulated saccade response with a fixation at $\theta_H = -15$ deg $\theta_V = 15$ deg. The left subplot represents the simulated generalized coordinates; the middle the coordinate speeds; right the estimated EOMs activations.

Bibliography

S.-h. Lee and D. Terzopoulos, "Heads Up ! Biomechanical Modeling and Neuromuscular Control of the Neck," *ACM Transactions on Graphics*, vol. 1, no. 212, pp. 1188–1198, 2006.

S. L. Delp, F. C. Anderson, A. S. Arnold, P. L. Loan, A. Habib, C. T. John, E. Guendelman, and D. G. Thelen, "OpenSim : Open-Source Software to Create and Analyze Dynamic Simulations of Movement," *IEEE Transactions on Biomedical Engineering*, vol. 54, no. 11, pp. 1940–1950, 2007.

D. A. Robinson, D. M. O'meara, A. B. Scott, and C. C. Collins, "Mechanical components of human eye movements," *Journal of Applied Physiology*, vol. 26, no. 5, pp. 548–553, 1969.

C. C. Collins, M. R. Carlson, a. B. Scott, and a. Jampolsky, "Extraocular muscle forces in normal human subjects." *Investigative ophthalmology & visual science*, vol. 20, no. 5, pp. 652–664, 1981.

J. Iskander, M. Hossny, S. Nahavandi, L. del Porto, and L. Porto, "An ocular biomechanic model for dynamic simulation of different eye movements," *Journal of Biomechanics*, 2018.

D. A. Robinson, "The mechanics of human saccadic eye movement," *The Journal of physiology*, pp. 245–264, 1964.

D. A. Robinson and A. F. Fuchs, "Eye movements evoked by stimulation of frontal eye fields." *Journal of Neurophysiology*, vol. 32, no. 5, pp. 637–648, 1969.

D. G. Thelen, F. C. Anderson, and S. L. Delp, "Generating dynamic simulations of movement using computed muscle control," *Journal of Biomechanics*, vol. 36, no. 3, pp. 321–328, mar 2003.

M. Millard, T. Uchida, A. Seth, and S. L. Delp, "Flexing computational muscle: modeling and simulation of musculotendon dynamics," *Journal of Biomechanical Engineering*, vol. 135, no. 2, pp. 1–12, mar 2013.

S. S. James, C. Papapavlou, A. Blenkinsop, A. J. Cope, S. R. Anderson, K. Moustakas, and K. N. Gurney, "Integrating brain and biomechanical models-A new paradigm for understanding neuro-muscular control," *Frontiers in Neuroscience*, vol. 12, no. FEB, 2018.

R. Kono, R. A. Clark, and J. L. Demer, "Active pulleys: Magnetic resonance imaging of rectus muscle paths in tertiary gazes," *Investigative Ophthalmology and Visual Science*, vol. 43, no. 7, pp. 2179–2188, 2002.